Fate of biomass inorganic elements during hydrothermal carbonisation: an experimental study on several agrofood waste

Julie Michel, Maria José Rivas Arrieta, Eleonora Boren, Loic Simonin, Maria Kennedy, Capucine Dupont

Biomass Conversion and Biorefinery
https://doi.org/10.1007/s13399-023-05105-9

ORIGINAL ARTICLE

Fate of biomass inorganic elements during hydrothermal carbonization: an experimental study on agro-food waste

Julie Michel[1,2] · María J. Rivas-Arrieta[1] · Eleonora Borén[3] · Loïc Simonin[2] · Maria Kennedy[1] · Capucine Dupont[1]

Received: 31 August 2023 / Revised: 1 November 2023 / Accepted: 2 November 2023

Abstract

The distribution of inorganic elements between solid and liquid phases during biomass hydrothermal carbonization (HTC) is a poorly investigated topic despite its importance for process optimization. To fill in this gap, the distribution of inorganic elements and their forms were determined for three agro-food waste feedstocks converted at HTC temperatures of 180, 220, and 260 °C in 12 h. Satisfactory balances were achieved, with values between 80 and 92% for C and N, and 80 and 110% for most inorganic elements. At 180 °C, over 90% of P, Mg, Ca, K, Na, and Mn were removed from hydrochars whatever feedstock. At higher temperatures, P, Mg, Ca, and Mn were partly reincorporated into hydrochars (between 7 and 53%), possibly due to the formation of insoluble precipitates, while K and Na remained in the liquid. On the opposite, some minor elements, Cu and Al, remained in the hydrochars, whatever temperature. Si showed different removal behaviors according to feedstock and temperature. These results show the possibility of optimizing the removal of inorganic elements from hydrochars using different temperatures.

Keywords Hydrothermal carbonization · Biochar · Elemental balances · Waste · Biomass · Inorganic elements

1 Introduction

In recent years, bioeconomy has emerged, prompting the recovery of abundant biomass waste from industry, agriculture, and forestry, thereby reincorporating them following a circular economy approach [1]. As biomass waste comprises a wide range of materials, they exhibit highly heterogeneous physicochemical properties, varying according to biomass type and origin. As comprehensively reviewed in [2], biomass waste contains variable amounts of organics and inorganics; the first includes mainly cellulose, hemicellulose, and lignin, while the latter is constituted by ash-forming elements such as Ca, K, Si, Mg, P, Na, and also heavy metals.

The most widely employed thermochemical conversion processes for biomass upgrading are combustion, gasification, pyrolysis, and hydrothermal conversion (carbonization, liquefaction, gasification—by order of increasing temperature severity [3]). Unlike the former processes, hydrothermal conversion allows for direct processing of high-moisture content biomass, typically operating in a range of 5 to 20% biomass-to-water ratio (B/W), and avoids the energy-intensive drying step. Hydrothermal conversion thus targets largely non-valorized wet biomass residual streams such as sludge, manure, and food waste; it can also be used with dry biomass with the addition of water. Hydrothermal carbonization (HTC) typically operates between 180 and 300 °C under autogenous pressure from 10 to 50 bars. Residence times can vary from one to several hours [4]. HTC typically gives rise to 35 to 80 weight-dry-basis (wdb)% of solid, commonly denoted as hydrochar, 20 to 65 wdb% liquid fraction containing water, organic and inorganic compounds, and 2 to 5 wdb% gas mainly consisting of CO_2 [4].

Hydrochars, like biochars from pyrolysis, have recently found many other applications besides their initial use as soil-improving material and solid fuel [5]. Among these

Julie Michel and María J. Rivas-Arrieta are equal contributors.

✉ Capucine Dupont
c.dupont@un-ihe.org

[1] Department of Water Supply, Sanitation and Environmental Engineering, IHE Delft, Westvest 7, 2611 AX Delft, The Netherlands

[2] Univ Grenoble Alpes, CEA, LITEN, DEHT, 38000 Grenoble, France

[3] Department of Chemistry, Umeå University, KBC-Huset (KB), Linnaeus Väg 10, Umeå Universitet, 901 87 Umeå, Sweden

Published online: 23 November 2023

applications, hydrochars are tested as adsorbent in water treatment of both organic and inorganic pollutants as well as in gas treatment of aromatic and polyaromatic hydrocarbons [6], or as carbon electrode in supercapacitors and batteries [5, 7]. However, depending on the application, the content of inorganic elements may be an issue, since they may adversely affect the final properties of the products. For instance, heavy metal content limits the application of hydrochar as a soil amendment material [8]. In other applications, such as electrodes for Na-ion batteries, Si and Ca seem to lower the performances [9, 10]. Using suitable processing routes that provide adequate separation or fractionation, the inorganic elements may be extracted or relatively enriched in an upgraded product, that is, the properties of the biomass waste may be tailored for a specific application.

Implementing a pretreatment step to extract inorganic elements may be crucial, particularly using biomass with high inorganic content. HTC has been evaluated as a means to remove inorganics, by extracting several inorganic elements to the processed liquid. Until now, research has often aimed at investigating P speciation and nutrient recovery for soil application from manure/sludge sources [11–13]. Wu et al. [13] determined that the reaction temperature was the only parameter significantly affecting the distribution of P, K, and N in the HTC products of cattle manure treated between 150 and 270 °C, from 0.5 to 6 h, and B/W from 0.025 to 0.125. Temperatures above 240 °C increased the concentration of nutrients in the hydrochar, while lower temperatures (150 °C) promoted their dissolution into the liquid. Similarly, Ghanim et al. [11] stated that increasing the reaction temperature leads to a higher P concentration in the hydrochars, particularly at temperatures ≥ 200 °C, whatever the residence time, which ranged between 5 and 480 min, resulting in the formation of primarily inorganic P species and P associations with Ca, Mg, Al, and Fe, which have also been found more abundant in the hydrochar with increasing temperatures [14].

Few articles have focused on a comprehensive study of the distribution of the inorganic elements during HTC with different biomass types. So far, only two articles have examined the fate of Si, Fe, Al, and Mn in addition to P, Ca, Mg, and K, using the inductively coupled plasma (ICP) method for measurement [15, 16]. Both measured the concentration of inorganic elements in the feedstock and resulting hydrochars, but not in the liquid fractions. Therefore, they could not establish any elemental balance. Note that it is assumed here that under HTC conditions, inorganic elements are not volatilized in the gas fraction. Their experiments showed that HTC seems to be an effective process to mobilize inorganic elements from biomass and that the temperature can be optimized to target specific elements. However, the results were obtained for short residence times of 5 min and 1 h and it is hazardous to extrapolate them at longer residence times used in HTC. Mechanisms were hypothesized to explain the observations, but without really discussing the differences in behavior between feedstocks. The authors suggest that knowing the inorganic compounds in the solid—and not only the inorganic element concentration—would be required for that purpose.

Based on this background, this experimental study aims to complement the existing information on inorganic element behavior during HTC by quantifying major and minor inorganic elements in both solid and liquid phases of HTC and therefore establishing for the first time elemental balances. For that purpose, HTC experiments were performed on three abundant agro-food wastes in a broad range of temperatures and for long residence times of 12 h. In addition, an attempt was made to go beyond the analysis in terms of elemental composition only and characterize the inorganic compounds in the feedstock and resulting hydrochars via X-ray diffraction (XRD) measurements. Based on these results, mechanisms were suggested to explain the behaviors observed for the different elements versus feedstock and temperature, and a discussion was made on the process implications of those results.

2 Materials and methods

2.1 Biomass feedstocks

Three agro-food wastes were selected based on their large availability in Europe. Apple waste was provided as pomace from the apple juice factory Värmdö Musteri AB, Sweden. Brewery waste was provided from Trondheim, Norway. Coffee material was spent grounds from the regular coffee shop "Barista," Sweden. Samples were obtained from Biokol Sverige AB, Sweden. They were received dried and milled below 1 mm. Drying was performed only for the practicality of the study, to make transportation and storage easier before experiments. Drying would not be necessary in HTC industrial process, as it can convert high-moisture materials. Water was added to the samples again for the HTC tests to keep a constant biomass-to-water ratio (Section 2.2.).

The moisture content of the materials was measured according to the standard UNE-EN 14774–2:2010, in order to account for internally bound moisture when determining B/W during HTC.

2.2 HTC experiments

The HTC experiments were conducted in duplicates in a 2-L high-pressure floor stand Parr reactor, series 4530, USA. For each run, 65 g dry basis (db) of biomass and 1300 mL demineralized water were fed to the reactor to achieve a 5% B/W, apart from the 260 °C run of apple waste where 49 g

db was used due to material shortage but still maintaining a 5% B/W. Before the experimental runs, the reactor was purged with N_2 for 2–3 min to inert the headspace. The reactor was heated at 2 °C/min until the desired temperature (180, 220, or 260 °C) and kept at that temperature for 12 h. A U-shaped stirrer was used at a rate of 100 rpm to agitate the reactor. The maximum autogenous pressure reached in each run is given in Table S1 of Supplementary Materials.

At the end of the experiment, the reactor was let to cool down naturally overnight. Gas samples were taken in duplicates while the rest of the gas was vented off. The HTC hydrochar and liquid were separated using a series of sieves of 100, 45, and 20 µm. The retained hydrochar was rinsed with about 500 mL of demineralized water and dried overnight at 70 °C. The sieved liquid fraction was filtrated through 0.45-µm acetate-cellulose filters, firstly pre-rinsed with demineralized water and secondly with the processed liquid before collecting the liquid samples.

Herein, the obtained product fractions are denoted "XT-p"; X is the initial letter of the biomass used as a feedstock (A, B, C), T is the HTC temperature, and p is the phase whether h for hydrochar or l for liquid.

2.3 Characterization of biomass and HTC products

2.3.1 Ash content and elemental characterization

Organic elements were determined differently in the different phases of the products. CHNS content of the solids was determined according to ISO 16948. Oxygen was obtained by difference between the total sample and C, H, N, S, and ash. Total organic carbon (TOC) and total nitrogen (TN) of the liquids were carried out by a Shimadzu TOCv-cpn analyzer. Gas composition was determined using a SCION 456-GC gas chromatograph with helium as a carrier gas; the oven column temperature was between 25 and 28 °C in all the measurements. The thermal conductivity detector (TCD) temperature was 140 °C, while the electron capture detector (ECD) temperature was 250 °C.

Ash content analysis of the solids was performed according to ISO 18122:2015.

The contents of Al, Ba, Ca, Fe, Mg, K, Na, Cr, Cu, Mn, Ni, and Sr in the raw biomass, hydrochar, and HTC liquid products were determined by inductively coupled plasma optical emission spectroscopy (ICP-OES), PerkinElmer, Avio 200. The digestion procedure for the solid samples was adapted from the standards ISO 16967 for the determination of major elements (Al, Ca, Fe, Mg, K, and Na) and ISO 16968 for the determination of minor elements (Ba, Cr, Cu, Mn, Ni, and Sr). The raw biomass and hydrochars were microwave digested (Mars 5 Duo Temp CEM microwave oven), adding 10 mL of 65% concentrated nitric acid to approximately 0.5 g of dried sample. The samples were heated at 165 °C for 10 min at 1600 W; the temperature was maintained 1 min and increased again at 175 °C for 5 min. The liquid samples were adjusted to match the 5% nitric acid background of the calibration and rinsing solutions of the spectrometer.

In the liquid samples, the P content was determined by inductively coupled plasma mass spectrometry (ICP-MS), Thermo Fisher XSeries II. The samples were prepared by adding four drops of concentrated sulfuric acid to 10 mL of HTC liquid, previously filtrated using 0.45-µm cellulose-acetate membrane filters, to obtain a 1% sulfuric acid concentration. Due to experimental constraints in the laboratory, another method, also well-validated, was used for the raw biomass and hydrochars. Samples were digested using sulfuric acid, selenium, salicylic acid, and hydrogen peroxide, as described in [17]. The P content was measured by colorimetry using a UV/VIS Lambda 365 Spectrophotometer, PerkinElmer, at a wavelength of 880 nm using the molybdenum blue method [17]. To ensure the consistency between the results for solids via UV/VIS and liquids via ICP-MS, some solid digestates could be characterized both by UV/VIS ICP-MS. The relative difference between measurements on the same sample using the two methods was below 10%.

The analyses of the raw biomass and hydrochars were carried out in triplicates, while the analysis of the liquid fraction was carried out in duplicates.

The quantification of Si in raw biomass and hydrochars was carried out by dissolving between 15 and 50 mg ash (according to standard ISO 18122:2015) in 1.5 g sodium hydroxide melt over a burner. Demineralized water of 400 mL and 20 mL 1:1 hydrochloric acid solution were added to the ash solution to form a silicic acid solution, which was used for the colorimetric determination of the Si content at 650 nm via the molybdenum blue complex, using a UV/VIS Lambda 365 Spectrophotometer, PerkinElmer, following the procedure described in [15] based on [18]. The analyses were carried out in duplicates.

All the values presented correspond to the mean and standard error of the mean.

2.3.2 Structural characterization

The structure of the biomass and hydrochars was analyzed by XRD using a D8 Advance Bruker AXS diffractometer with a copper cathode ($\lambda K\alpha = 15{,}418$ Å). The 2θ angle was varied from 5° to 80° using a step size of 0.05° and a counting time of 1 s. The different organic and inorganic crystalline phases were identified with the PDF4 + database supplied by the ICDD. Phase identification was made using EVA software.

2.3.3 pH measurement

The pH of the liquid product was measured using a pH 3310 WTW precision meter. Measurements were conducted in duplicates after filtration of the liquid.

2.3.4 Macromolecular composition

Cellulose and hemicellulose were measured using a method adapted from TAPPI standard T249 cm-85, and lignin using TAPPI standard T222 om-83–1988. Extractives were measured by gravimetry, after extraction successively by hot water and acetone under pressure. The methods are described in detail in [10].

2.3.5 Scanning electron microscopy–energy-dispersive X-ray spectroscopy (SEM–EDS)

Observations were performed in a Zeiss LEO 1530 Field Emission Gun SEM microscope with a Bruker EDS detector. EDS cartographies were performed with a 20 kV operating voltage with a 10 mm working distance. The materials were coated with 20 nm of carbon, by a CCU-010 SAFEMATIC Eden Instrument.

2.4 Calculations

The solid yield was calculated according to Eq. 1:

$$\text{solid yield} = \frac{\text{hydrochar mass}}{\text{raw material mass}} \times 100 \quad (1)$$

With solid yield expressed in w%, and hydrochar mass and raw material mass in kg.

To compare the results, the content units were converted in mg per kg of raw biomass on dry basis (mg/kg raw db) according to Eq. 2 for hydrochars and Eq. 3 for liquids.

$$hydrochar\ content_{rawdb} = hydrochar\ content \times solid\ yield \quad (2)$$

where hydrochar content $_{\text{raw db}}$ is in mg/kg raw db, the hydrochar content is the element mass in the hydrochar in mg/kg db, and solid yield is in w%.

$$liquid\ content_{rawdb} = concentration_{final} \times DL \times \frac{V_{initial}}{m_{rawbiomass}} \quad (3)$$

where liquid content $_{\text{raw db}}$ is in mg/kg dry db, concentration $_{\text{final}}$ the element concentration in the liquid in mg/L, DL the dilution factor (no unit), $V_{initial}$ the volume of water introduced in the reactor (L), and $m_{\text{raw biomass}}$ the mass of feedstock filled in the reactor in kg db.

It should be noted that, as explained in previous studies [7], the total liquid yield can only be calculated by difference with solid and gas yields; it is therefore not presented as a result. In addition, when calculating the concentration of elements in the liquid, the assumption was made that the volume of liquid produced during HTC was negligible compared to the initial volume of water added in the reactor (1.3 L). This assumption seems reasonable since the feedstock mass was around 0.06 kg, and assuming it would be fully converted into a liquid of 1 kg/L density, the volume produced would represent 0.06 L, that is, less than 5% of the initial volume.

3 Results and discussion

3.1 HTC product mass yields

Solid yields are reported in Table 1. As explained in Sect. 2.4, they represent the ratio of the final dried hydrochar mass to the initial biomass mass in wdb%.

Hydrochar yields varied between 36 and 51 wdb%, the remaining being mostly liquid, with a few percent of gas. The increase in temperature favored the production of liquid and gas at the expense of hydrochar, which showed a decrease in yield of around 10% in absolute between values at 180 and 260 °C. Such results are consistent with HTC literature under these conditions [4]. The relatively low hydrochar yields are logical considering the long residence times as well as the feedstocks, which are not lignin-rich lignocellulosic biomass compared with wood, as it is reported in Table 2—lignin being known to hardly degrade under HTC conditions. Interestingly, the yields were almost the same for brewery and apple waste but higher for coffee waste. This difference is obviously related to the composition of this feedstock, discussed in terms of elements in the sections below.

3.2 Organic component analyses and distribution

The elemental composition is reported in Table 1 for both feedstocks and hydrochars.

Carbon contents in the raw biomass are 42.8 wdb% (apple waste) and 50.3 wdb% (coffee waste), which represents a high fraction of the materials. The values for H and N vary from 6.9 wdb% (apple waste) to 7.8 wdb% (coffee waste), and from 0.6 wdb% (apple waste) to 3.3 wdb% (brewery waste), respectively. Sulfur contents of all feedstocks are below 0.3 wdb%, which is close to the detection limit. Such ranges of values are in agreement with what was found for similar feedstock [19–22] and lignocellulosic biomass in general [2, 23].

Table 1 Organic composition of the raw materials and products at different temperatures from the solid, liquid, and gas phase

	Solids							Liquids			Gas
	Solid yield	Ash	C	H	N	S	O (by difference)	pH	TOC	TN	CO_2
	wdb%	wdb%							mg/L		wdb%
Apple raw		2.4 ± 0.1	42.8 ± 0.1	6.9 ± 0.1	0.6 ± 0.0	0.3 ± 0.1	47.1	4.0 ± 0.1			
180 °C	47 ± 1	0.3 ± 0.1	61.2 ± 1.2	6.1 ± 0.0	1.0 ± 0.0	0.1 ± 0.0	31.4	3.4 ± 0.1	2900 ± 100	40 ± 7	2.0 ± 0.1
220 °C	42 ± 1	0.3 ± 0.1	69.7 ± 0.9	5.6 ± 0.1	1.1 ± 0.0	0.1 ± 0.0	23.3	3.8 ± 0.1	2700 ± 500	38 ± 10	4.05 ± 0.01
260 °C	38 ± 1	0.6 ± 0.1	75.1 ± 0.2	5.7 ± 0.2	1.1 ± 0.0	0.1 ± 0.0	17.4	4.0 ± 0.1	5000 ± 1000	80 ± 20	5 ± 2
Brewery raw		3.6 ± 0.1	46.1 ± 0.2	7.2 ± 0.1	3.3 ± 0.0	0.2 ± 0.0	39.5	4.1 ± 0.1			
180 °C	45 ± 1	0.9 ± 0.1	63.2 ± 0.3	7.0 ± 0.1	3.2 ± 0.0	0.3 ± 0.0	25.5	4.0 ± 0.1	6670 ± 70	930 ± 10	1.62 ± 0.02
220 °C	37 ± 1	0.5 ± 0.1	71.5 ± 0.5	7.1 ± 0.1	3.9 ± 0.0	0.3 ± 0.0	16.7	4.4 ± 0.1	6660 ± 10	875 ± 3	3.74 ± 0.02
260 °C	36 ± 1	0.9 ± 0.1	76.0 ± 0.0	7.3 ± 0.0	4.1 ± 0.0	0.2 ± 0.0	11.5	5.0 ± 0.1	5790 ± 30	884 ± 8	5.29 ± 0.03
Coffee raw		2.1 ± 0.1	50.3 ± 0.3	7.8 ± 0.0	2.4 ± 0.1	0.1 ± 0.0	37.2	5.9 ± 0.1			
180 °C	52 ± 1	0.3 ± 0.1	64.7 ± 0.9	8.0 ± 0.1	2.5 ± 0.0	0.2 ± 0.0	24.4	3.9 ± 0.1	6390 ± 10	514 ± 7	1.1 ± 0.1
220 °C	46 ± 1	0.5 ± 0.1	72.5 ± 0.5	8.0 ± 0.1	2.9 ± 0.1	0.2 ± 0.0	15.8	4.4 ± 0.1	5700 ± 40	482 ± 1	3.3 ± 0.3
260 °C	42 ± 1	0.6 ± 0.1	76.0 ± 0.2	8.3 ± 0.1	3.0 ± 0.0	0.1 ± 0.0	12	4.9 ± 0.1	4980 ± 9	492 ± 0	4.6 ± 0.7

Table 2 Macromolecular composition of the raw biomass in wdb%

Macromolecule composition, wdb%	Apple waste	Brewery waste	Coffee waste
Lignin	12 ± 1	17 ± 1	23.3 ± 0.6
Extractives	48 ± 4	30.0 ± 0.6	22 ± 1
Sugars			
Glucose	18 ± 2	16.5 ± 0.4	8.68 ± 0.00
Xylose	3.11 ± 0.08	12.1 ± 0.3	0.27 ± 0.02
Mannose	1.23 ± 0.04	0.63 ± 0.04	22.6 ± 0.3
Galactose	2.3 ± 0.2	0.91 ± 0.01	11 ± 2
Arabinose	3.9 ± 0.8	7.04 ± 0.07	2.32 ± 0.06
Total cellulose	16 ± 2	15.8 ± 0.3	-
Total hemicellulose	14 ± 1	22.6 ± 0.4	-

The organic composition of hydrochars and liquids is reported in Table 1. The distribution of the amount of C and N contained in the feedstock and the products is shown in Fig. 1.

The elemental balances, expressed in weight percentage, could be carried out for C and N. In both cases, they were between 80 and 90% for C recovery and 87 to 92% for N recovery. Such values are similar to those found in the same set-up in [7]. This closure can be considered satisfactory for such a type of experiment and the missing elements may be explained by several sources of experimental errors, as discussed in detail in [7].

As expected, hydrochars displayed lower H:C and O:C ratios than the feedstock, due to dehydration and decarboxylation reactions, and C content increased with increasing reaction temperature [15]. Overall, the C content of the hydrochars ranged from 61 to 76 wdb%, which

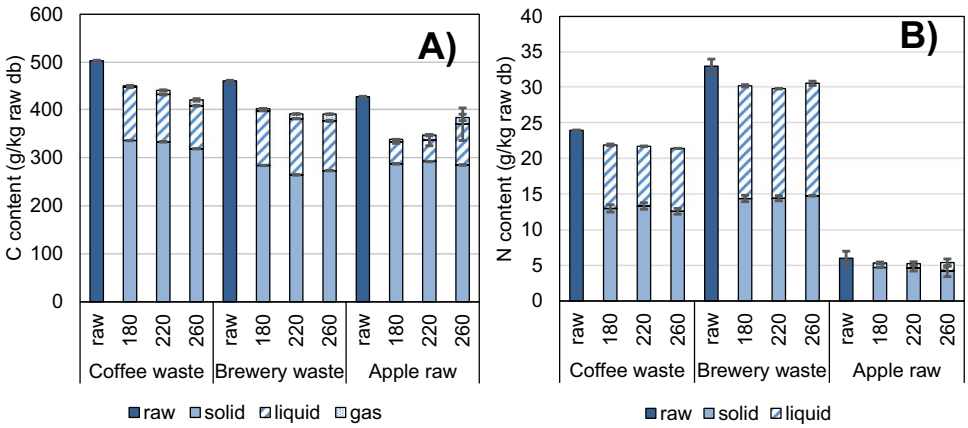

Fig. 1 Carbon (**A**) and nitrogen (**B**) balances at the different temperatures for the solid, liquid, and gas fractions. The values were converted to grams of element per kilogram of raw biomass dry basis. Carbon in the liquid is calculated from the total organic carbon of the total C. Carbon in the gas phase is deduced from the produced CO_2. Nitrogen in the liquid is deduced from the measured total nitrogen. Standard deviations are experimental between the replicates

agrees with typical values from literature. More detailed comparisons with HTC experiments led on similar feedstock look hazardous due to the different operating conditions used, notably the residence time [24–27]. Notably, at the highest temperature of 260 °C, C content was approximately 76 wdb% for the three hydrochars, whatever the initial C content (42–50 wdb%) in the feedstock.

The C content in the liquid after reaction is assimilated to the TOC content. While it slightly decreases with temperature from 6670 to 5800 mg/L for brewery waste and 6390 to 4980 mg/L for coffee waste, it significantly increases from 2900 to 5300 mg/L for apple waste. Other authors have reported a decrease with temperature for digestate and manure [28]. A high TOC at lower reaction temperatures can indicate hydrolysis reactions taking place and releasing organic compounds into the liquid, such as organic acids. A further reduction of the TOC could indicate polymerization reactions [25]. The increase observed for apple waste has no obvious explanation and might be due to experimental errors.

A small portion of the initial C introduced, less than 4%, ends in the gas phase, mainly composed of CO_2. As the temperature increases, the quantity of CO_2 produced increases for all feedstocks, from 1–2 wdb% of the initial dry biomass at 180 °C to 5 wdb% at 260 °C. Such results are in accordance with results obtained on the same set-up [7]. They can be explained by the decarboxylation reactions that occur above 180 °C from the degradation of carboxyl and carbonyl groups and lead to CO_2 and CO production, respectively [29, 30].

The N content decreased for the three samples with respect to the raw biomass and increasing reaction temperature. Such result is in agreement with the measurements in [15] for some of their samples, but not all, the trends being apparently feedstock-dependent. However, one should keep in mind that the values measured are low and, in some cases, such as the apple-based materials, close to the detection limit.

The S content, as discussed above, was around the detection limit in the biomass samples and was also logically found around this limit in the hydrochars.

3.3 Inorganic element analysis and distribution

Ash contents are reported in Table 1, while inorganic contents of solids and liquids are reported in Table 3 and Table 4, respectively. The distribution of inorganics between hydrochar and liquid is represented in Fig. 2, Fig. 3, and Fig. 4 for apple, brewery, and coffee materials, respectively.

3.3.1 Ash content

The range of values in the three biomass samples was between 2.1 and 3.6 wdb%, which is relatively moderate,

Table 3 Inorganic composition of the solids: raw biomass and hydrochars in mg/kg db. Standard deviations are experimental between the replicates. Hydrochars are called by the first letter of the raw material (A for apple, B for brewery waste, or C for coffee) followed by the HTC temperature (180, 220, or 260), and the suffix -h

	P	K	Na	Ca	Mg	Sr	Al	Cu	Cr	Mn	Fe	Ba	Ni	Si
	mg/kg db													
Apple raw	960 ± 70	7350 ± 30	76 ± 4	756 ± 1	501 ± 1	1.92 ± 0.04	11.4 ± 0.4	3.9 ± 0.5	< 1	6.10 ± 0.01	18.4 ± 0.8	< 1	< 60	80 ± 10
A180-h	149 ± 7	812 ± 8	< 10	80 ± 2	29 ± 2	< 1	9 ± 1	7.1 ± 0.6	< 1	< 1	90 ± 10	< 1	< 60	157 ± 9
A220-h	220 ± 10	585 ± 2	< 10	210 ± 30	35 ± 3	< 1	16 ± 1	8.5 ± 0.5	6 ± 1	3.2 ± 0.4	135 ± 1	< 1	< 60	160 ± 10
A260-h	830 ± 40	580 ± 100	< 10	1000 ± 200	140 ± 30	2.0 ± 0.7	24 ± 3	10.4 ± 0.5	11 ± 3	9 ± 2	250 ± 20	< 1	< 60	100 ± 20
Brewery raw	4590 ± 30	776 ± 2	407 ± 1	1720 ± 30	1870 ± 20	12.6 ± 0.1	12 ± 2	10.6 ± 0.1	< 1	32.3 ± 0.2	73 ± 3	4.5 ± 0.3	< 60	5300 ± 300
B180-h	420 ± 40	< 30	20 ± 1	290 ± 5	125 ± 9	< 1	8 ± 1	24.2 ± 0.3	5.2 ± 0.6	5.2 ± 0.2	198 ± 2	< 1	< 60	2500 ± 100
B220-h	470 ± 20	< 30	15 ± 2	560 ± 30	117 ± 5	3.0 ± 0.2	8.3 ± 0.9	26.1 ± 0.3	50 ± 20	10.0 ± 0.3	340 ± 30	< 1	< 60	420 ± 60
B260-h	1210 ± 30	< 30	13 ± 1	1170 ± 70	370 ± 30	7.9 ± 0.4	13.3 ± 0.7	23.1 ± 0.8	42 ± 1	15.9 ± 0.6	410 ± 10	6 ± 5	< 60	800 ± 100
Coffee raw	710 ± 30	8350 ± 50	200 ± 20	880 ± 10	1170 ± 20	2.6 ± 0.1	6 ± 2	20.0 ± 0.2	< 1	14.0 ± 0.3	25 ± 3	< 1	< 60	17 ± 8
C180-h	110 ± 30	740 ± 60	26 ± 4	110 ± 10	123 ± 5	< 1	9 ± 1	42 ± 2	3 ± 1	5.19 ± 0.06	116 ± 8	< 1	< 60	8.3 ± 0.4
C220-h	680 ± 40	430 ± 10	18 ± 2	1020 ± 50	205 ± 4	1.9 ± 0.1	12.9 ± 0.8	44.4 ± 0.3	16 ± 2	16.5 ± 0.4	168 ± 2	< 1	< 60	37 ± 7
C260-h	810 ± 50	640 ± 50	40 ± 10	820 ± 50	201 ± 5	1.7 ± 0.2	17 ± 2	44 ± 1	60 ± 6	12 ± 1	424 ± 5	< 1	< 60	37.1 ± 0.9

Table 4 Inorganic composition of the liquids. They are presented in mg/L for P, K, Na, Ca, and Mg, and in µg/L for Sr, Al, Cu, Cr, Mn, Fe, Ba, and Ni. Standard deviations are experimental between the replicates. Liquids are called by the first letter of the raw material (A for apple, B for brewery waste, or C for coffee) followed by the HTC temperature (180, 220, or 260), and the suffix -l

	P	K	Na	Ca	Mg	Sr	Al	Cu	Cr	Mn	Fe	Ba	Ni
	mg/L					µg/L							
A180-l	33.3 ± 0.7	358 ± 0	3.33 ± 0.09	34.9 ± 0.7	22.1 ± 0.1	129 ± 3	41 ± 3	80 ± 20	3.1 ± 0.8	305 ± 9	1000 ± 200	108 ± 2	200 ± 50
A220-l	30.1 ± 0.4	352 ± 5	3.03 ± 0.08	26.70 ± 0.08	20.1 ± 0.2	105 ± 1	36.1 ± 0.3	48 ± 9	< 2	243 ± 8	900 ± 300	92.6 ± 0.5	590 ± 60
A260-l	20 ± 2	352 ± 1	3.01 ± 0.01	11 ± 3	14.4 ± 0.4	50 ± 10	50 ± 20	12 ± 4	< 2	240 ± 20	5610 ± 20	49 ± 6	300 ± 50
B180-l	138 ± 1	37.6 ± 0.3	16.7 ± 0.1	74 ± 1	82.0 ± 0.3	567 ± 4	60 ± 1	130 ± 10	14.8 ± 0.7	1310 ± 20	2660 ± 40	402 ± 2	1080 ± 60
B220-l	140 ± 6	37.6 ± 0.3	16.8 ± 0.1	65.0 ± 0.5	80.9 ± 0.2	499 ± 2	46 ± 1	11.9 ± 0.9	14 ± 2	1260 ± 20	3900 ± 200	354 ± 2	990 ± 20
B260-l	134 ± 8	38.2 ± 0.3	16.9 ± 0.1	49.2 ± 0.1	74 ± 1	379 ± 1	43 ± 1	< 2	8.97 ± 0.05	1230 ± 10	3200 ± 300	291 ± 4	970 ± 20
C180-l	20.3 ± 0.1	393 ± 3	8.8 ± 0.1	38.4 ± 0.2	50.9 ± 0.6	149 ± 1	39 ± 2	220 ± 40	6 ± 2	550 ± 10	90 ± 20	85.8 ± 0.9	180 ± 30
C220-l	9.8 ± 0.7	401 ± 2	9.3 ± 0.1	14.7 ± 0.8	49.1 ± 0.2	84 ± 1	19.1 ± 0.5	19.8 ± 0.7	2.3 ± 0.2	310 ± 30	8 ± 2	65.9 ± 0.4	< 120
C260-l	7 ± 2	403 ± 2	9.2 ± 0.1	14 ± 2	46.1 ± 0.4	62 ± 8	19 ± 4	< 2	< 2	490 ± 30	2000 ± 100	35 ± 3	< 120

and aligned with literature on similar feedstock [19, 20, 31].

The ash content in the hydrochars was systematically lower than in the feedstock, with a decrease between 0.3 wdb% (C180-h and A220-h) and 0.9 wdb% (B180-h). Such a decrease is significant, as the experimental uncertainty is ± 0.1 wdb%. It means that less than a third of the ash content of the corresponding feedstock remains in the hydrochars.

Both C180-h and A180-h have an ash content of 0.3 wdb%, which increases to 0.6 wdb% at 260 °C. The trend is different for brewery waste, with the lowest ash content of 0.5 wdb% measured at the intermediate temperature of 220 °C, while for 180 and 260 °C, the ash content was significantly higher (0.9 wdb%). Afolabi et al. [24] obtained hydrochars of spent coffee grains in which the ash content only slightly varies between an initial value of 1.2 to 1.0 wdb% at 180 °C and 1.3 wdb% at 220 °C and 5 h residence time (considering the same uncertainty of measurement as in the present study, ± 0.1 wdb%). In other studies, ash of apple pomace hydrochars has been reported as low as 0.02 wdb%—the initial feedstock containing 2 wdb% ash—at intermediate temperatures of 220–225 °C, but has increased to 1.5 wdb% at a higher temperature of 260 °C [27], which is also the case for brewery waste. It is logical not to find clear trends valid for all feedstocks, since ash content is a lumped value. It is particularly useful to define the material suitability as solid fuel, but hides the relevant parameters here. Indeed, ash content is determined by the content in different inorganic elements, susceptible to behave differently—and interact—during the HTC process. These latter measurements are presented and discussed below.

3.3.2 Closure of the elemental balances

The elemental balance, expressed in weight percentage, was found to be between 80 and 110% for the majority of the inorganic elements in all experiments. To our knowledge, no similar elemental balance on HTC experiments has been carried out previously. Such closure can be seen as satisfactory when compared with other experimental studies on inorganic element distribution in thermal processes, such as gasification [32]. For a few elements, in particular P, Cu, and Al, the closure was slightly less satisfactory though, between 64 and 87% for P, while for Cu and Al, the range was a bit broader, between 78 and 125%.

3.3.3 Inorganic element concentrations in feedstock

Raw coffee waste was found to be particularly rich in K, with a value higher than 8000 mg/kg db, and to a lower extent in

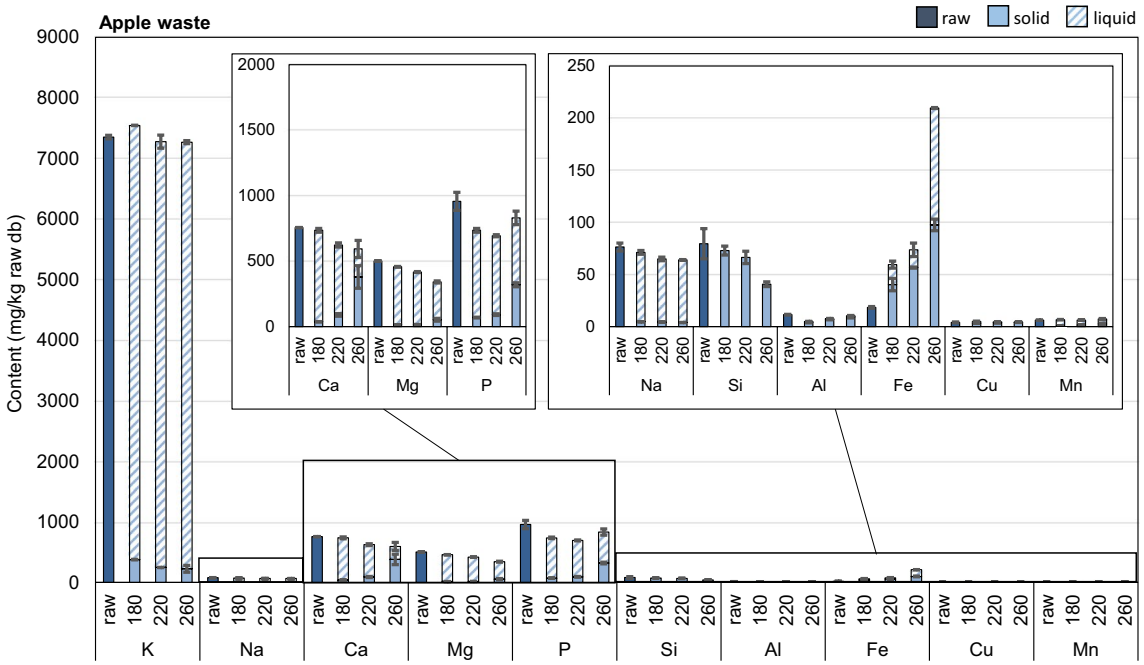

Fig. 2 Balance of the inorganics between the raw material and the hydrochar (solid) and liquid at the different temperatures of 180, 220, and 260 °C from apple waste. The different elements were represented on different scale, depending on the content. The values were converted on milligram of element per kilogram of raw biomass in order to compare them together. Standard deviations are experimental between the replicates

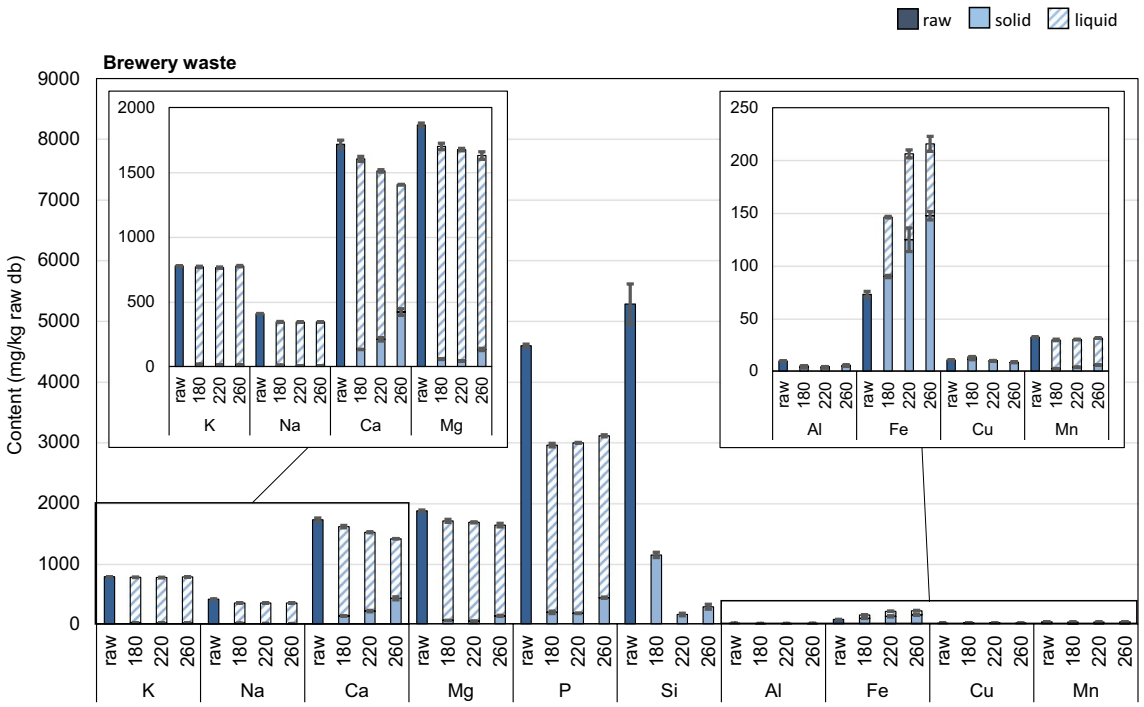

Fig. 3 Balance of the inorganics between the raw material and the hydrochar (solid) and liquid at the different temperatures of 180, 220, and 260 °C from brewery waste. The different elements were represented on different scale, depending on the content. The values were converted on milligram of element per kilogram of raw biomass in order to compare them together. Standard deviations are experimental between the replicates

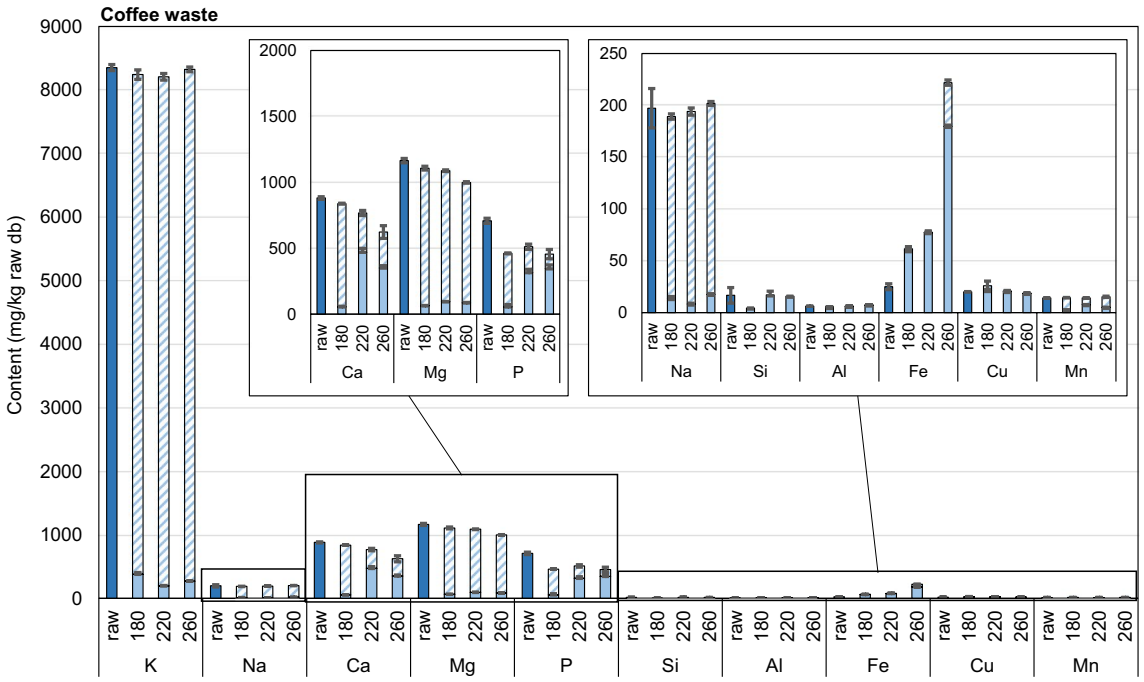

Fig. 4 Balance of the inorganics between the raw material and the hydrochar (solid) and liquid at the different temperatures of 180, 220, and 260 °C from coffee waste. The different elements were represented on different scale, depending on the content. The values were converted on milligram of element per kilogram of raw biomass in order to compare them together. Standard deviations are experimental between the replicates

Mg, with a value slightly higher than 1000 mg/kg db, and Ca and P, with values a bit lower than 1000 mg/kg db. Similar orders of magnitude have been found in previous studies on similar feedstock [33, 34]. Ballesteros et al. [33] also measured significant amounts of Ba, Co, and Ni, which was not the case in our sample. Such differences, and in general differences in the overall composition of spent coffee grounds, are not surprising and can be explained by the diversity in origins, soil chemistry, processing, and extraction methods used to obtain the final coffee product.

Similarly, apple waste appeared to be specifically rich in K, with a value of around 7350 mg/kg db. Ca, Mg, and P were again the other main elements, with values between 500 and 1000 mg/kg db. Such values seem in agreement with Skinner et al. [35], who reviewed apple pomace compositions in these ranges.

Contrary to the other feedstocks, brewery waste showed a high content of Si, with a value of around 5300 mg/kg db. Its P content was also found in a similar high range, with around 4500 mg/kg db, while Ca and Mg were also present, in slightly lower but still high amounts, with values close to 2000 mg/kg db. Significant concentrations of K and Na were found too, with values of several hundred mg/kg db. The Ca content is in accordance with [36] but not the concentrations of Si, Mg, and P, lower in their case. The high Si content seems logical as the parent material of brewery waste consists of barley and its husks. Indeed, plants are known to take Si from the soil in the form of silicic acid, which then accumulates around cellulose micropores of the husks in the form of nanoparticles [37].

All feedstocks also showed Al, Cu, Fe, Mn, and Sr traces. The concentrations were similar, with values ranging from 2 to 30 mg/kg db, except in the case of brewery waste, slightly richer in Fe, with values close to 100 mg/kg db. Such values agree with literature [38]. Values were found to be below the detection limit for As, Cd, Cr, Ni, Pb, and Ba—for this latter, except in brewery waste, the value remaining however small (4.5 mg/kg db).

3.3.4 Major inorganic elements in HTC products

K and Na were mainly present in the liquid product, whatever temperature and feedstock, as highlighted in Fig. 2, Fig. 3, and Fig. 4. About 1 to 4% of K and Na remained in the solid phase for all the experiments, in accordance with other HTC experiments using different biomass types such as swine manure [28] and sea lettuce [39]. According to Smith et al. [15], K and Na are present in biomass as ionic salts ($NaNO_3$, KNO_3, NaCl, and KCl). As these alkali metal salts are readily soluble in water, their large decrease in the hydrochars was expected. Moreover, the acidic conditions given by the initial feedstock and the HTC process benefit

hydrolysis reactions, thus promoting the removal of K and Na. Indeed, the pH of the reaction liquids was acidic. In general, the pH of the HTC liquid product increased with increasing reaction temperature. Despite the differences in initial pH for coffee and brewery waste, their HTC liquid had an almost identical pH between 3.9 (C180-l) and 5.0 (B260-l) after reaction at each temperature. On the other hand, all the HTC products obtained from apple waste revealed a more acidic pH between 3.4 (A180-l) and 4.0 (A260-l). Such acidic values are overall in agreement with literature, but, as discussed above, it is questionable to make more detailed comparisons with previous studies on similar feedstocks [25, 26], due to the different operating conditions. These acidic values can be partly explained by the hemicellulose degradation from HTC temperatures of about 180 °C and the associated production of low molecular weight acids like acetic, formic, lactic, levulinic, and propionic [25]. Subsequently, as temperature increases, pH increases due to the re-polymerization of these intermediate products dissolved in the liquid phase into the solid phase.

On the contrary to K and Na, the distribution of Ca, Mg, and P between solid and liquid varied with temperature in the range tested, and that for all feedstocks. At 180 °C, only 3 to 8% (respectively for Mg in A180-h and P in C180-h) of Ca, Mg, and P remained in the hydrochars. However, as temperature increased, between 7 and 53% of Ca, Mg, and P were found in the hydrochars (for respectively P in B220-h and Ca in C220-h), which means there was a higher retention of these elements at higher temperature. For P, the retention was the highest at 260 °C for all feedstock. Such a result extends the trend observed in [15] from 200 to 250 °C. However, an exception could be seen for coffee waste hydrochars, which retained more Ca and Mg at 220 °C than at 260 °C.

As the organic matter is initially hydrolyzed at the lowest HTC temperatures, organic P has been shown to dissolve into the processed liquid, where organic functional groups may be substituted by metals, forming inorganic phosphorous species that precipitate back to the solid phase [40]. This process may be prompted at higher process temperatures, leading to the accumulation of some P in the hydrochars. Increasing temperature also promotes an increase in pH, as observed in the present experiments. This prompts the precipitation of P, mainly as orthophosphates, with some metals, such as alkaline earth metals Ca and Mg [12]. Such a mechanism may explain why their concentration in the hydrochars also increases with increasing temperature for brewery and apple waste hydrochars. Ghanim et al. [11] suggested that P precipitates mainly consist of Mg and Ca phosphates and apatite ($Ca_5(PO_4)_3(F, Cl, OH)$).

Ca and Mg in lignocellulosic biomass can be present as ionic salts, a minority incorporated into macromolecules, and for Ca, the remaining fraction is predominantly in the form of calcium oxalate, an acid-soluble compound [41]. Therefore, the initial acidic and subcritical water conditions may have promoted some Ca migration into the processed liquid at 180 °C. Ca is also found, along with Mg and Mn, in the biomass cell walls, possibly bonded to carboxyl groups, which are degraded under HTC conditions via decarboxylation. This fraction of Ca, Mg, and Mn is thought to be ion-exchangeable [41]. Consequently, Ca could be liberated only to be re-adsorbed by the remaining or newly formed functional groups on the surface of hydrochars, which may enhance their cation exchange capacity [15].

The content of Si was measured on the feedstock and hydrochars only, as the method is not suitable for liquids. Si showed a large decrease compared to the raw biomass for brewery waste. This decrease was favored by the increase in temperature. Indeed, 22% of Si remained in the hydrochars at 180 °C (B180-h), while merely 3 and 5% remained at 220 and 260 °C (B220-h and B260-h) respectively. For apple waste hydrochars, the Si content also decreased with temperature, retaining 92% Si at 180 °C (A180-h) and 51% at 260 °C (A260-h). The trend seemed the opposite with coffee waste hydrochars, Si being more retained at higher temperatures. However, this trend must be taken with caution due to the low initial Si content of the raw coffee waste (17 mg/kg db), close to the limit of detection estimated for the method when considering blank samples (8 mg/kg db).

Overall, these results are consistent with previous findings in which HTC was proven effective in leaching Si out of the biomass structure. For instance, Smith et al. [15] found that around 20% of Si remained in willow hydrochars at 200 °C and Poerschmann et al. [42] determined that around 50% of Si present in brewery waste was extracted at 200 and 240 °C. However, for other biomass types rich in Si, such as rice hulls (36,000 mg/kg), sewage sludge (332,400 mg/kg), and digestate (67,100 mg/kg), several authors found little or no Si removal under HTC conditions [15, 16, 43]. For instance, rice hull hydrochars retained 80% Si at 200 °C and 74% at 260 °C, while digestate released around 15% Si at 190 °C but the element was reincorporated again at 250 °C.

These differences suggest that Si extraction from the solid matrix may depend on the relative chemical stability in which it is present within the biomass matrix. As suggested in [16], Si is very stable in rice hulls as silica hydrate, which provides rigidity to the plant, or is linked with covalent bonds to organic materials, or present as extraneous minerals such as quartz and clay [2], which tend to be even more thermally stable at the range of HTC temperatures. Si can also be dissolved as $Si(OH)_4$ in plant tissues [44], which may be easier to extract during HTC. Furthermore, hop is biochemically degraded during the brewery process, which might lead to more accessible Si species.

As a complement to the bulk elemental analyses, the SEM–EDS pictures—given as Supplementary Material

S2 to S10—seem to show that whatever the feedstock and hydrochars, the distribution of elements is homogenous, without any preferential location for the inorganics.

3.3.5 Minor inorganic elements in HTC products

Other elements, such as Al and Fe, remained mainly in the hydrochars for all the tested temperatures and feedstocks.

Most Cu initially present in the biomass remained in the solid phase after HTC. Some Cu seems to be extracted at 260 °C for coffee and brewery waste, but no significant concentrations were found in the liquid fraction to close the balance. This latter result should be then taken with caution.

Mn showed a similar behavior as Ca and Mg, with a large release in liquid at 180 °C and reincorporation into the solid phase at 220 and 260 °C. The element Sr seemed to follow the same behavior too, but those results should be taken cautiously considering the very small amount of Sr present in the feedstock, especially in the case of coffee and apple waste. Mn could be released from the biomass matrix early in the HTC process during hydrolysis when the protein complexes break down [45]. The further accumulation of Mn in the solid phase could be explained by its association with P as a precipitate, classified as non-apatite inorganic P, as suggested in [12].

It must be noted that the content of Fe, Cr, and Ni in the hydrochar and liquid products exceeded the amount of these elements fed to the reactor for all experiments. For instance, Fe content of the hydrochars was between 240 and 720% for coffee waste, 120 and 200% for brewery waste, and 220 and 530% for apple waste, with respect to the initial concentrations in the raw biomass. Such values are thought to be due to the leaching of Fe from the reactor made up of stainless steel grade 316, as shown by additional tests performed using demineralized water (see Supplementary Material S11). The values measured for Cr and Ni may therefore have the same explanation, even if for those two elements, the initial amounts in the raw biomass were close to the limit of detection. Thus, the results should be considered with caution.

3.4 XRD analyses on feedstock and hydrochars

The XRD patterns are shown in Fig. 5 for the feedstock and hydrochars produced at different temperatures.

Raw apple waste presents three broad peaks at around 15, 23, and 35°. They are typically observed for lignocellulosic biomass and are generally attributed to semi-crystalline cellulose [46]. These peaks, which remain at 180 °C, tend to disappear at higher process temperatures, logically indicating the decomposition of this form of cellulose. The increase of peak intensity between the raw material and the hydrochar obtained at 180 °C could come from the degradation of the amorphous compounds, such as hemicelluloses, at this temperature. It is indeed known that hemicelluloses begin to be hydrolyzed at 180 °C while cellulose requires a higher temperature above 220 °C to be significantly degraded [29].

The raw coffee waste shows a different feature than raw apple waste, between 15° and 25°. Indeed, besides the typical bump observed for apple waste, sharper peaks, which are difficult to explain, appear at 16, 20, 21, and 25°. However, these sharp peaks could also be observed in literature for spent coffee grounds [33, 47]. XRD patterns for coffee waste hydrochars showed the presence of n-heneicosane (PDF 00–031-1705) from 180 °C and for all the HTC temperatures studied. Its presence is much less obvious in the raw biomass; however, it could be masked by the presence of other amorphous compounds that are decomposed after HTC. Heneicosane has been detected in fresh and fermented coffee beans [48] and is known to naturally occur in certain plants as a waxy solid [49].

The raw brewery waste XRD shows a less defined crystalline cellulose feature. It can be explained by the fact that brewery waste results from the fermentation of barley, inducing degradation of the cellulose. This cellulose structure seems to reappear at 180 °C, which can also be attributed to the degradation of the other amorphous compounds. A sharp peak at 21° appears at a higher temperature (260 °C) that can be attributed to silicate (SiO_2 cristobalite beta, syn, PDF 01–077-8630). Indeed, this feedstock had the highest Si content, and while Si was largely removed from solid, the amount remaining in hydrochar may be sufficient for detection in XRD. Silicon oxide compounds have also been detected in hydrochars derived from sugarcane bagasse [14] and algal biomass [50].

3.5 Synthesis of the results

Figure 6 summarizes the trends observed regarding inorganics' behavior during HTC for the three biomass types studied and the related mechanisms in the solid and liquid phases. Note that these mechanisms may vary when considering other operating conditions than those tested, as well as other biomass types, because the inorganic elements may be present in different forms and thus behave differently during HTC.

An important aspect is that no single trend is valid for all inorganics. Such a result explains the lack of agreement between authors about the influence of HTC on ash content from different feedstocks.

Mechanisms of release/reincorporation of inorganics from/in the solid vary in the temperature range considered, including solubilization of salts for release and precipitation for reincorporation. Those mechanisms are influenced by the degradation of the organic matter, in particular via the acidic conditions created by hemicellulose degradation into

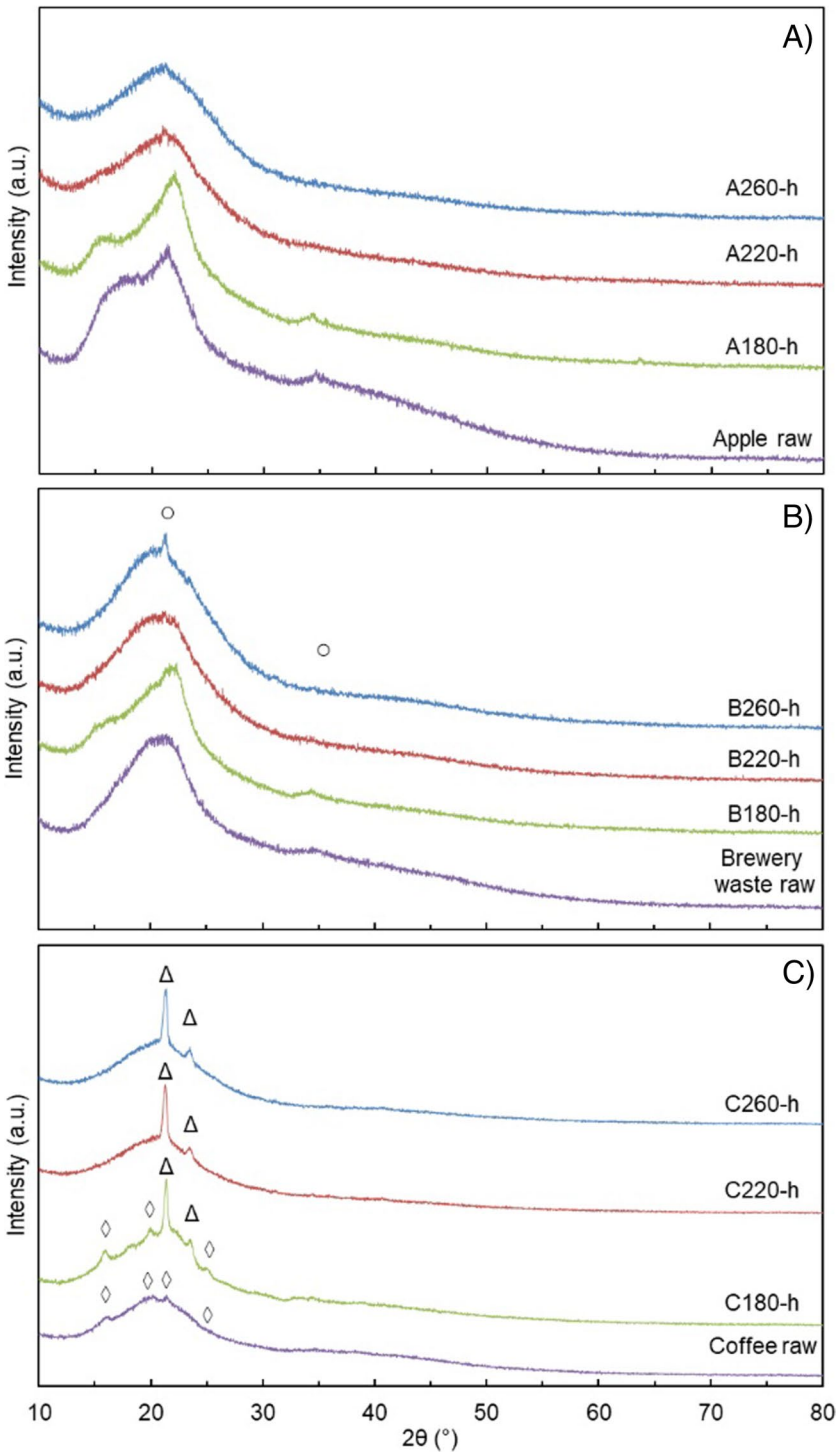

Fig. 5 XRD patterns of **A** apple waste–based materials, **B** brewery waste–based materials, and **C** coffee waste–based derivate materials. Structures of Δ $C_{21}H_{44}$ n-heneicosane (PDF 00–031-1705) and ○ SiO_2 silicon oxide, cristobalite beta, syn (PDF 01–077-8630) are represented. ◊ indicates unidentified peaks

organic acids, and a concentration effect, as inorganics will be more concentrated inside the solid after the degradation of some organic matter in it.

In the range of temperatures tested, high temperature does not seem to be beneficial in terms of inorganic release. The lowest temperature tested is the one at which more inorganic elements are released. At higher temperatures, while some inorganic elements, such as K and Na, continue to be released, others, such as Ca, Mg, or P, tend to be reincorporated into the solid.

The optimal temperature depends on the inorganic elements sought to be released, which depends on the application of the hydrochars and/or the liquids produced. In addition, releasing inorganics from the solid

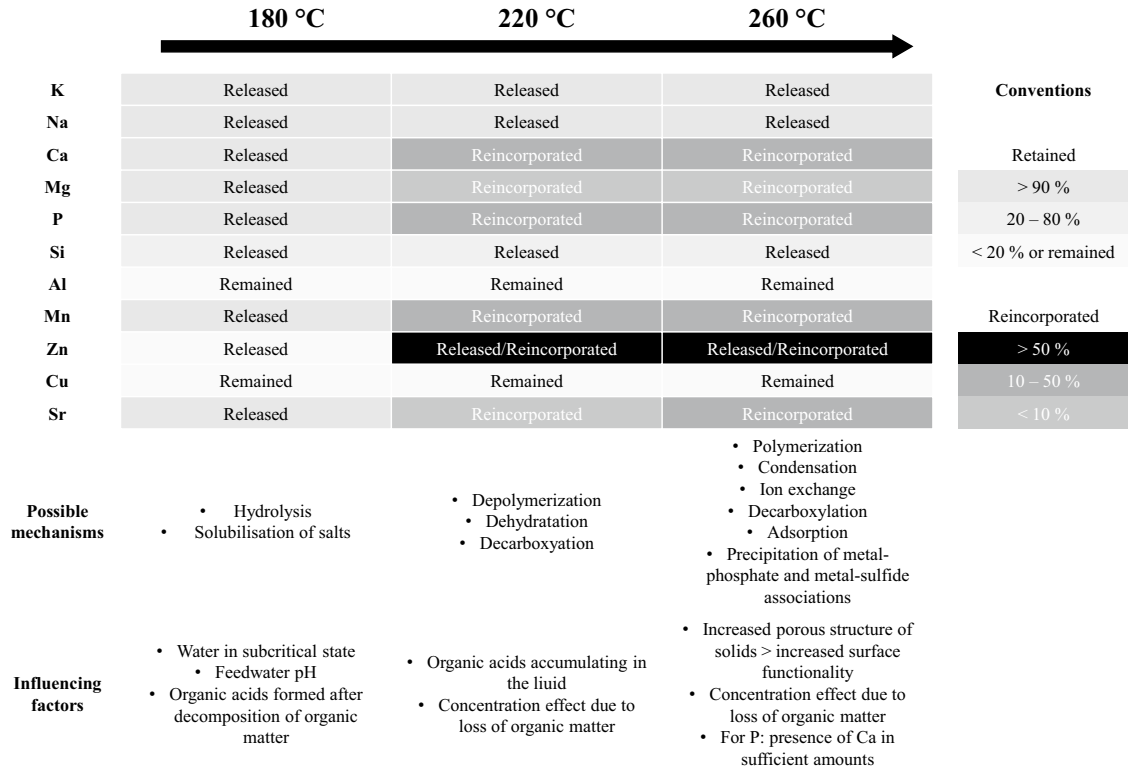

Fig. 6 Identified reaction mechanisms participating in the distribution of inorganic elements during HTC of coffee, brewery, and apple waste for 12 h as a function of reaction temperatures of 180, 220, and 260 °C

fraction may be one objective of the HTC treatment but not the only one, and the HTC process may be part of a value chain consisting of several treatments. A compromise may therefore need to be found in terms of optimal temperature depending on the other properties targeted and the combination with downstream treatments. Typically, if the final product is intended to be used in Na-ion batteries, the focus would be on removing Ca and Si, known to decrease electrochemical performances [51]. A temperature of 180 °C could then be optimal, and the "clean" hydrochar would undergo post-treatment by high-temperature pyrolysis to be turned into a material having the required hard carbon structure [7].

As a final remark, one should keep in mind that the residence time influence was not tested here. The choice of 12 h was made to get an extreme case—the longest residence time possible considering the experimental constraints in the laboratory, but additional experiments would be required to investigate the inorganic distribution at intermediate residence times and check if there are observable differences and therefore room for optimization in a process viewpoint.

4 Conclusion

Although inorganic elements are determining properties for end-uses of HTC products, their distribution between solid and liquid versus feedstock and operating conditions remains overlooked in literature.

To fill in this gap, a systematic campaign of experiments was carried out in a 2-L reactor using three agro-food wastes and three temperatures covering the HTC range between 180 and 260 °C, with the focus put on closing the balances for both organic and inorganic elements.

Satisfactory balances were achieved, with values between 80 and 92% for C and N, and 80 and 110% for most inorganic elements, slightly less satisfactory values being obtained for P (64–87%) and Cu and Al (78–125%).

The experiments showed that whatever feedstock, a large amount (> 90%) of the inorganic elements initially present were released in the liquid phase at the lowest HTC temperature tested (180 °C). With increasing temperature, some reincorporation into the solid phase (between 7 and 53%) occurred for P, Mg, Ca, and Mn, while elements such as K and Na remained in the liquid, and Cu and Al remained in

the solid. Si behavior was more feedstock-dependent, showing a considerable extraction from the solids in brewery waste (up to 97%) and apple waste (up to 49%) but not in coffee waste. It was the only inorganic compound leading to crystalline structure (SiO_2) in the hydrochars.

From a process viewpoint, this study confirms that HTC can be a treatment step aiming to release inorganics from solid and turn them into the liquid phase. For that purpose, low temperatures such as 180 °C appear optimal; however, other criteria may need to be considered when optimizing the process, particularly the other properties targeted for the products.

Supplementary information The online version contains supplementary material available at https://doi.org/10.1007/s13399-023-05105-9.

Acknowledgements The authors acknowledge Despoina Andriotou from CEA for the SEM-EDX pictures, Malte Lilliestråle from Biokol Sverige AB for supplying the samples of raw biomass, and the assistance of IHE lab staff.

Author contribution JM: conceptualization, methodology, formal analysis, laboratory investigation, data curation, writing—original draft, and visualization.

EB: conceptualization, methodology, validation, supervision, and writing - review and editing.

LS: conceptualization, methodology, resources, validation, supervision, and writing - review and editing.

CD: conceptualization, methodology, resources, validation, supervision, and writing - review and editing.

Funding This work was co-funded by the European Union's Horizon 2020 research and innovation program NAIMA under grant agreement no. 875629 and the Erasmus Mundus.

Data availability All data can be made available upon reasonable request to the authors.

Declarations

Ethical approval Not applicable.

Competing interests The authors declare no competing interests.

References

1. Ubando AT, Felix CB, Chen WH (2020) Biorefineries in circular bioeconomy: a comprehensive review. Biores Technol 299:122585
2. Vassilev SV, Baxter D, Andersen LK, Vassileva CG, Morgan TJ (2012) An overview of the organic and inorganic phase composition of biomass. Fuel 94:1–33. https://doi.org/10.1016/j.fuel.2011.09.030
3. Yang C, Wang S, Yang J, Xu D, Li Y, Li J, Zhang Y (2020) Hydrothermal liquefaction and gasification of biomass and model compounds: a review. Green Chem 22:8210–8232. https://doi.org/10.1039/d0gc02802a
4. Yoganandham ST, Sathyamoorthy G, Renuka RR (2020) Emerging extraction techniques: hydrothermal processing, in: Sustainable seaweed technologies. Elsevier Inc., 191–205. https://doi.org/10.1016/b978-0-12-817943-7.00007-x
5. Nicolae SA, Au H, Modugno P, Luo H, Szego AE, Qiao M, Li L, Yine W, Heeres HJ, Berge N, Titirici MM (2020) Recent advances in hydrothermal carbonisation: from tailored carbon materials and biochemicals to applications and bioenergy. Green Chem 22(15):4747–4800
6. Sharma HB, Sarmah AK, Dubey B (2020) Hydrothermal carbonization of renewable waste biomass for solid biofuel production: a discussion on process mechanism, the influence of process parameters, environmental performance and fuel properties of hydrochar. Renew Sustain Energy Rev 123:109761
7. Qatarneh AF, Dupont C, Michel J, Simonin L, Beda A, Matei Ghimbeu C, Ruiz-Villanueva V, da Silva D, Piégay H, Franca MJ, Bedal A, MateiGhimbeu C, Ruiz-Villanueva V, da Silva D, Piégay H, Franca MJ (2021) River driftwood pretreated via hydrothermal carbonization as a sustainable source of hard carbon for Na-ion battery anodes. J Environ Chem Eng 9:106604. https://doi.org/10.1016/j.jece.2021.106604
8. European Biochar Foundation (2016) Guidelines for a sustainable production of biochar. European Biochar Foundation (EBC). https://www.european-biochar.org/media/doc/2/version_en_9_5.pdf
9. Correa CR, Hehr T, Voglhuber-Slavinsky A, Rauscher Y, Kruse A (2019) Pyrolysis vs. hydrothermal carbonization: understanding the effect of biomass structural components and inorganic compounds on the char properties. J Anal Appl Pyrol 140:137–147
10. Rios CMS (2020) Study of biomass-derived hard carbons for Sodium-ion battery application. Chemical and Process Engineering. Thesis, Université Grenoble Alpes
11. Ghanim BM, Kwapinski W, Leahy JJ (2018) Speciation of nutrients in hydrochar produced from hydrothermal carbonization of poultry litter under different treatment conditions. ACS Sustain Chem Eng 6:11265–11272. https://doi.org/10.1021/acssuschemeng.7b04768
12. Shi Y, Chen Z, Cao Y, Fan J, Clark JH, Luo G, Zhang S (2021) Migration and transformation mechanism of phosphorus in waste activated sludge during anaerobic fermentation and hydrothermal conversion. J Hazard Mater 403:123649. https://doi.org/10.1016/j.jhazmat.2020.123649
13. Wu K, Zhang X, Yuan Q (2018) Effects of process parameters on the distribution characteristics of inorganic nutrients from hydrothermal carbonization of cattle manure. J Environ Manage 209:328–335. https://doi.org/10.1016/j.jenvman.2017.12.071
14. Silva CC, Melo CA, Soares Junior FH, Moreira AB, Ferreira OP, Bisinoti MC (2017) Effect of the reaction medium on the immobilization of nutrients in hydrochars obtained using sugarcane industry residues. Bioresour Technol 237:213–221. https://doi.org/10.1016/j.biortech.2017.04.004
15. Smith AM, Singh S, Ross AB (2016) Fate of inorganic material during hydrothermal carbonisation of biomass: influence of feedstock on combustion behaviour of hydrochar. Fuel 169:135–145. https://doi.org/10.1016/j.fuel.2015.12.006
16. Reza MT, Lynam JG, Uddin MH, Coronella CJ (2013) Hydrothermal carbonization: fate of inorganics. Biomass Bioenerg 49:86–94. https://doi.org/10.1016/j.biombioe.2012.12.004

17. Walinga I, Van der Lee JJ, Houba VJG, Van Vark W, Novozamsky I (1995) Plant analysis manual, Plant analysis manual. Springer Dordrecht. https://doi.org/10.1007/978-94-011-0203-2
18. Vogel AI (1989) Vogel's textbook of quantitative chemical analysis, Fifth edit. ed. Longman Scientific & Technical. https://doi.org/10.1038/100304b0
19. Cerino-Córdova FJ, Dávila-[17] Walinga I, Van der Lee JJ, Houba VJG, Van Vark W, Novozamsky I (1995) Plant analysis manual, Plant analysis manual. Springer Dordrecht. https://doi.org/10.1007/978-94-011-0203-2
20. Coronado MA, Montero G, Montes DG, Valdez-Salas B, Ayala JR, García C, Carrillo M, León JA, Moreno A (2020) Physicochemical characterization and SEM-EDX analysis of brewer's spent grain from the craft brewery industry. Sustainability 12:7744. https://doi.org/10.3390/su12187744
21 Gowman AC, Picard MC, Rodriguez-Uribe A, Misra M, Khalil H, Thimmanagari M, Mohanty AK (2019) Physicochemical analysis of apple and grape pomaces. BioResources 14:3210–3230. https://doi.org/10.15376/biores.14.2.3210-3230
22. Kang SB, Oh HY, Kim JJ, Choi KS (2017) Characteristics of spent coffee ground as a fuel and combustion test in a small boiler (6.5 kW). Renew Energy 113:1208–1214. https://doi.org/10.1016/j.renene.2017.06.092
23. Da Silva Perez D, Dupont C, Guillemain A, Jacob S, Labalette F, Briand S, Marsac S, Guerrini O, Broust F, Commandre JM (2015) Characterisation of the most representative agricultural and forestry biomasses in France for gasification. Waste Biomass Valorization 6:515–526. https://doi.org/10.1007/s12649-015-9374-3
24. Afolabi OOD, Sohail M, Cheng YL (2020) Optimisation and characterisation of hydrochar production from spent coffee grounds by hydrothermal carbonisation. Renew Energy 147:1380–1391. https://doi.org/10.1016/j.renene.2019.09.098
25. Arauzo PJ, Olszewski MP, Kruse A (2018) Hydrothermal carbonization brewer's spent grains with the focus on improving the degradation of the feedstock. Energies 11:3236. https://doi.org/10.3390/en11113226
26. Suárez L, Benavente-Ferraces I, Plaza C, de Pascual-Teresa S, Suárez-Ruiz I, Centeno TA (2020) Hydrothermal carbonization as a sustainable strategy for integral valorisation of apple waste. Biores Technol 309:123395. https://doi.org/10.1016/j.biortech.2020.123395
27. Zhang B, Heidari M, Regmi B, Salaudeen S, Arku P, Thimmannagari M, Dutta A (2018) Hydrothermal carbonization of fruit wastes: a promising technique for generating hydrochar. Energies 11:1–14. https://doi.org/10.3390/en11082022
28. Ekpo U, Ross AB, Camargo-Valero MA, Williams PT (2016) A comparison of product yields and inorganic content in process streams following thermal hydrolysis and hydrothermal processing of microalgae, manure and digestate. Biores Technol 200:951–960. https://doi.org/10.1016/j.biortech.2015.11.018
29. Funke A, Ziegler F (2010) Hydrothermal carbonization of biomass: a summary and discussion of chemical mecha- nisms for process engineering. Biofuels Bioprod Biorefin 4:160–177. https://doi.org/10.1002/bbb.198
30. Wang T, Zhai Y, Zhu Y, Li C, Zeng G (2018) A review of the hydrothermal carbonization of biomass waste for hydrochar formation: process conditions, fundamentals, and physicochemical properties. Renew Sustain Energy Rev 90:223–247. https://doi.org/10.1016/j.rser.2018.03.071
31. Lyu F, Luiz SF, Azeredo DRP, Cruz AG, Ajlouni S, Ranadheera CS (2020) Apple pomace as a functional and healthy ingredient in food products: a review. Processes 8:1–15. https://doi.org/10.3390/pr8030319
32. Defoort F, Dupont C, Durruty J, Guillaudeau J, Bedel L, Ravel S, Campargue M, Labalette F, Da Silva Perez D (2015) Thermodynamic study of the alkali release behavior during steam gasification of several biomasses. Energy Fuels 29(11):7242–7253
33. Ballesteros LF, Teixeira JA, Mussatto SI (2014) Chemical, functional, and structural properties of spent coffee grounds and coffee silverskin. Food Bioprocess Technol 7(12):3493–3503. https://doi.org/10.1007/S11947-014-1349-Z
34. Mussatto SI, Carneiro LM, Silva JPA, Roberto IC, Teixeira JA (2011) A study on chemical constituents and sugars extraction from spent coffee grounds. Carbohyd Polym 83:368–374. https://doi.org/10.1016/j.carbpol.2010.07.063
35. Skinner RC, Gigliotti JC, Ku KM, Tou JC (2018) A comprehensive analysis of the composition, health benefits, and safety of apple pomace. Nutr Rev 76:893–909. https://doi.org/10.1093/nutrit/nuy033
36 Khidzir KM, Abdullah N, Agamuthu P (2010) Brewery spent grain: chemical characteristics and utilization as an enzyme substrate. Malaysian J Sci 29:41–51
37. Liu N, Huo K, McDowell MT, Zhao J, Cui Y (2013) Rice husks as a sustainable source of nanostructured silicon for high performance Li-ion battery anodes. Sci Rep 3:1–7. https://doi.org/10.1038/srep01919
38. Bowen HJM (1966) Trace elements in biochemistry. Academic Press, London
39. Shrestha A, Acharya B, Farooque AA (2021) Study of hydrochar and process water from hydrothermal carbonization of sea lettuce. Renew Energy 163:589–598. https://doi.org/10.1016/j.renene.2020.08.133
40. Deng Y, Zhang T, Clark J, Aminabhavi T, Kruse A, Tsang DCW, Sharma BK, Zhang F, Ren H (2020) Mechanisms and modelling of phosphorus solid-liquid transformation during the hydrothermal processing of swine manure. Green Chem 22:5628–5638. https://doi.org/10.1039/d0gc01281e
41. Khazraie Shoulaifar T, Demartini N, Zevenhoven M, Verhoeff F, Kiel J, Hupa M (2013) Ash-forming matter in torrefied birch wood: changes in chemical association. Energy Fuels 27:5684–5690. https://doi.org/10.1021/ef4005175
42. Poerschmann J, Weiner B, Wedwitschka H, Baskyr I, Koehler R, Kopinke FD (2014) Characterization of biocoals and dissolved organic matter phases obtained upon hydrothermal carbonization of brewer's spent grain. Biores Technol 164:162–169. https://doi.org/10.1016/j.biortech.2014.04.052
43. Zhao X, Becker GC, Faweya N, Rodriguez Correa C, Yang S, Xie X, Kruse A (2018) Fertilizer and activated carbon production by hydrothermal carbonization of digestate. Biomass Convers Biorefinery 8:423–436. https://doi.org/10.1007/s13399-017-0291-5
44. Boström D, Skoglund N, Grimm A, Boman C, Öhman M, Broström M, Backman R (2012) Ash transformation chemistry during combustion of biomass. Energy Fuels 26:85–93. https://doi.org/10.1021/ef201205b
45. Marzbali MH, Paz-Ferreiro J, Kundu S, Ramezani M, Halder P, Patel S, White T, Madapusi S, Shah K (2021) Investigations into distribution and characterisation of products formed during hydrothermal carbonisation of paunch waste. J Environ Chem Eng 9:104672. https://doi.org/10.1016/j.jece.2020.104672
46. Saavedra Rios CDM, Simonin L, De Geyer A, Ghimbeu CM, Dupont C (2020) Unraveling the properties of biomass-derived hard carbons upon thermal treatment for a practical application in Na-ion batteries. Energies 13:3513. https://doi.org/10.3390/en13143513
47. Block I, Günter C, Rodrigues AD, Paasch S, Hesemann P, Taubert A (2021) Carbon adsorbents from spent coffee for

removal of methylene blue and methyl orange from water. Materials 14:3996. https://doi.org/10.3390/ma14143996
48. Oliveira Junqueira AC, de Melo Pereira GV, Coral Medina JD, Alvear MCR, Rosero R, de Carvalho Neto DP, Enríquez HG, Soccol CR (2019) First description of bacterial and fungal communities in Colombian coffee beans fermentation analysed using Illumina-based amplicon sequencing. Sci Rep 9:1–10. https://doi.org/10.1038/s41598-019-45002-8
49. Vanitha V, Vijayakumar S, Nilavukkarasi M, Punitha VN, Vidhya E, Praseetha PK (2020) Heneicosane—a novel microbicidal bioactive alkane identified from Plumbago zeylanica L. Ind Crops Prod 154:112748. https://doi.org/10.1016/j.indcrop.2020.112748
50. de Castro JS, Assemany PP, de Carneiro ACO, Ferreira J, de Jesus Júnior MM, de Rodrigues FÁ, Calijuri ML (2021) Hydrothermal carbonization of microalgae biomass produced in agro-industrial effluent: products, characterization and applications. Sci Total Environ 768:144480. https://doi.org/10.1016/j.scitotenv.2020.144480
51. Rios CDMS, Simonin L, Ghimbeu CM, Vaulot C, da Silva Perez D, Dupont C (2022) Impact of the biomass precursor composition in the hard carbon properties and performance for application in a Na-ion battery. Fuel Process Technol 231:107223